

## Cold Spray Metallization of Hybrid Thermoplastic - Thermoset Fiber Reinforced Composite

Hetal Parmar<sup>1,a\*</sup>, Roberta Della Gatta<sup>2,b</sup>, Antonio Viscusi<sup>2,c</sup>, Fausto Tucci<sup>1,d</sup>,  
Antonello Astarita<sup>2,e</sup>, Pierpaolo Carlone<sup>1,f</sup>

<sup>1</sup>Department of Industrial Engineering, University of Salerno, Italy

<sup>2</sup>Department of Chemical, Materials and Production Engineering, University of Naples Federico II, Italy

<sup>a</sup>hparmar@unisa.it; <sup>b</sup>roberta.dellagatta@unina.it, <sup>c</sup>antonio.viscusi@unina.it, <sup>d</sup>ftucci@unisa.it,  
<sup>e</sup>antonello.astarita@unina.it, <sup>f</sup>pcarlone@unisa.it

**Keywords:** Metallization; cold spray; polymer matrix composites; cocuring; resin infusion

**Abstract.** Surface metallization is amongst the recent trends in the polymer and polymer matrix composites (PMCs) research industries to improve the electrical and thermal properties and exploit the subsequent utilization in the aerospace sector. Specifically, polymer matrix composites have been subjected to the limitations in form of high temperature exposure and substrate deterioration. The present study encompasses a new strategy in the manufacturing and metallization process. The first stage in the manufacturing of hybrid thermoplastic-thermoset composite was the hot compaction which comprised of primary preform preparation enabling the partial impregnation of the thermoplastic resin through the fabric reinforcement layer. The subsequent stage entailed the preform vacuum bagging and conducting catalyzed thermoset resin impregnation. The vacuum resin infusion step included a cocuring cycle to generate a fiber reinforced composite comprising of thermoplastic and impregnated thermoset resin with improved adhesion. Resin flow front movement was analyzed during the resin infusion process. Composite metallization was achieved through cold spray (CS). CS process parameters influence on the coating quality and characterization of laminates through microstructural analysis and results have been reported. The hybrid composite with thermoset resin through thickness and in-plane impregnation was achieved with the intact adherent thermoplastic layer after the curing cycle. In the CS metallization, the effective operative window of stand-off distances (SoD) and temperature has been determined.

### Introduction

The key industry sectors are seeking out advanced materials and advanced manufacturing techniques to build high performances components [1,2,11–16,3–10]. In the recent years, aerospace sector has been the recipient of several polymer and PMC materials system insertion primarily due to the advantages of weight reduction and high strength to weight ratio. Different metallization techniques have been employed to improve the electrical and thermal properties of PMCs. Major amongst them are electroless plating, physical vapor deposition (PVD), chemical vapor deposition (CVD) which have been observed to present different drawbacks in the metallization of PMCs [17]. Thermal spray technique consists of disadvantages involving the high temperature flames and deterioration of the substrate surface under the exposure of high temperature [18]. Cold spray (CS) process facilitates metallization in solid state avoiding the melting and is feasible for the low processing temperature materials polymers and PMCs [19–21]. Recent literature indicated the feasibility of metallization on the thermoplastic matrix substrate [22]. In case of thermoplastic polymers metallization, issues such as low coating adhesion in low pressure cold spraying (LPCS) was minimized by the insertion of interlayer strategy [23,24]. Several investigations focused on employing the CS variants for the deposition of Cu [23], Al [17], Sn [25], and Ti [26]. Effect of processing parameters on the CS coating was investigated in different investigations involving the CFRP, GFRP, and carbon fiber (CF)-PEEK composites as a substrate [27–29]. On the other hand, CS of thermoset PMCs involves issues such as matrix surface erosion and fiber exposure owing to

presence of the brittle matrix [30,31]. For instance, high pressure cold spraying (HPCS) of Al on CFRP with Epoxy matrix resulted in the CF fracture and substrate removal. Negative deposition efficiency (DE) was obtained in case of Cu and Fe HPCS on CFRP in the study undertaken by Che et al. [25]. Different strategies have been employed to overcome the issues concerning the thermoset metallization.

The “co-curing” strategy was employed in literature that included a thermoplastic coupling layer over the thermoset substrate which can be subjected to the cure together in order to realize a hybrid composite. Some investigations consisted this approach for the welding purpose [32,33]. In line with the similar concept, manufacturing of hybrid thermoset-thermoplastic composite utilizing the cocuring approach and further cold spraying was attempted as one of the potential strategy [34]. In this investigation, the hybrid thermoplastic layer was subjected to the co-curing with the CF reinforced thermoset infusion process in order to form a hybrid composite. CS as a potential metallization strategy was employed. A microstructural analysis was conducted in the manufacturing stage as well as the coating stage. Adhesion between the top layer and the substrate and the coating formed was considered as an important criterion and was assessed by the adhesion peel-off test. The findings along with the discussion has been included in the article.

## Materials and Method

The material selection for the experimental work was conducted from the advanced aerospace applications point of view. A high  $T_g$  (217°C) temperature amorphous thermoplastic PEI (ULTEM 1000) was utilized to form initial hybrid interlayer. The high-density aerospace application grade RTM6 epoxy resin was considered to form a thermoset resin infused composites.

**Manufacturing of the hybrid composite.** Resin infusion as an out of autoclave (OoA) route was considered in the manufacturing of the hybrid composites. As a primary stage, a hybrid interlayer was realized by the partial impregnation of the PEI resin through the CF reinforcement. Such partial flow in the fiber was promoted under the hot-pressing action (Fig. 1 a).

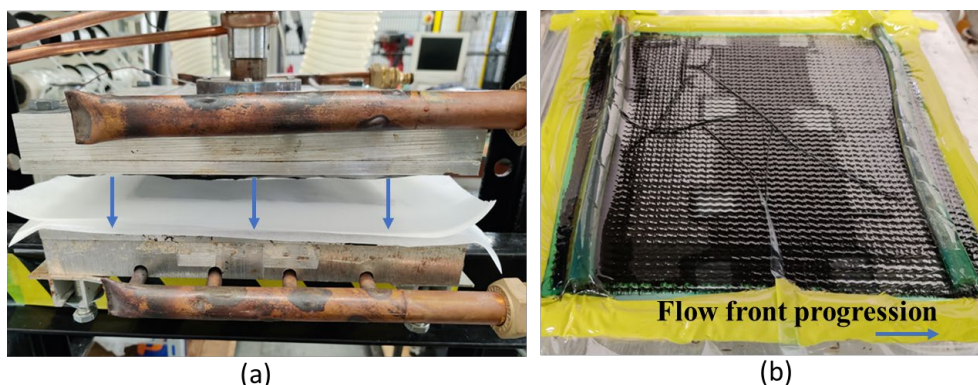


Fig. 1 (a) Hot compression process to realize the TP hybrid interlayer (b) Resin infusion set-up for hybrid composite manufacturing consisting of 8 CF layers.

The semi-preg was combined and stacked with the other CF reinforcing layers and auxiliary materials for vacuum bagging of the preform under negative pressure generation. The vacuum assisted resin infusion (VARI) process was followed by the curing stage (Fig. 1 b) The designated curing temperature 180°C for the Epoxy resin was attained under the two-stage curing cycle as also evidenced in literature for PEI-Epoxy interphase generation. Followed by the resin and mould preheating, resin infusion was conducted at 90°C temperature. Two hours of dwell time was maintained at the 180 °C curing temperature with the intermediate hold at 160°C temperature. Total of 12 resin infusion trials were realized to ensure repeatability in the assessment.

The manufactured composite panels were metalized by LPCS (courtesy, Sophia Tech. IT) under the variation in the processing parameters namely, gas temperature and stand-off distance (SoD). AlSi10Mg powder was utilized for the metallization of the composite surface. Three basic processing parameters were considered for the campaign, including gas temperature that was varied from

T2=240°C, T3=360°C, and T4=480°C. The stand of distance (SoD) between the nozzle orifice and the substrate to be sprayed was varied between 10, 15, 25, 35, and 45 mm. The cold spray chamber pressure was kept constant at 5.5 bar for each variation. The manufactured reference case and metallized composite panels were subjected to the microstructural analysis by the optical microscopy (OM) and further scanning electron microscopy (SEM). Prior to the OM observation, the samples were subjected to the metallographic specimen preparation according to the standard prescribed procedure. The samples were cut by the abrasive disc cutter and polished with the abrasive rough paper grades and fine polished subsequently. EDAX spectra were acquired to determine the elemental composition on specific areas of the coated samples.

Adhesion peel off test was conducted in order to assess the adhesion strength of the coated and uncoated composite specimens. During the peel off test, the cyanoacrylates adhesive applied over the sample surface and the test stub (dolly) with 10 mm diameter was attached over it. Required force for the complete debonding of the specimen and the stub was recorded. The failure surface over the coated and uncoated specimen were examined to study the failure condition and mode.

## Results and Discussion

**Analysis of manufactured hybrid composites.** In the primary stage of the hybrid interlayer formation, hot pressing action promoted the transverse flow of the PEI through the fiber layer. In order to generate a partially infused layer, the close control of the operating parameters such as the compression pressure, temperature and the hot press hold time is required. Partially impregnated hybrid PEI and CF interlayer was formed by the hot-pressing action at temperature of 235°C and pressure of 3.5 ton over the total mould surface area. The PEI polymer transversal flow into the inter-tow region of the fiber layer can be evidenced into Fig. 2. The hot press temperature higher than the PEI T<sub>g</sub> of 217°C resulted in the initiation of polymer flow. The uniform pressure distribution yielded close contact between the PEI and CF layer.

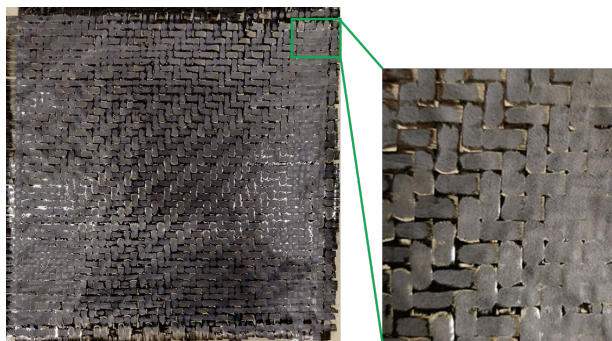


Fig. 2 Hot-pressed hybrid interlayer of PEI and CF.

Referring to the concept of the hybrid interlayer method of TS-TP composite manufacturing, it is necessary to provide non-wetted area for the further resin infusion of thermoset. The opposite side of the hot-pressed layer surface was kept not impregnated by the PEI.

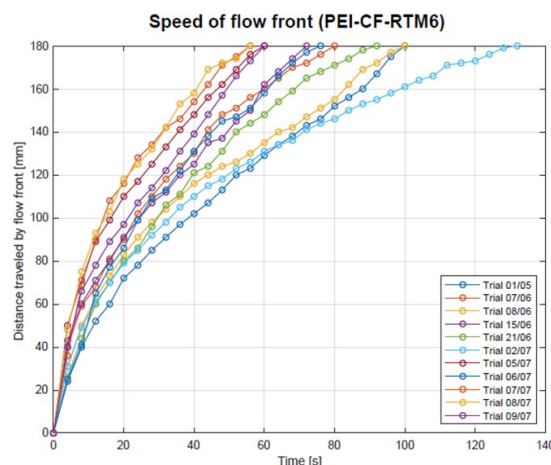


Fig.3 Resin flow front progression in experimental campaign.

During the resin infusion (RI) process, the RTM6 resin flow front progression was monitored during different trials and the relative data has been included in the Fig.3. It was observed to be linear, and the acquired micrographs (Fig. 4 a) indicated the in-plane and transversal flow of the resin through the fiber tows. The inter-tow regions of the fiber bundle were found to be filled with the resin percolated through the neatly placed distribution media. The resin viscosity was maintained by means of the indirect heating involving the heater to uniform temperature increase up to 80 °C temperature. The slight variation in can be due to the resin viscosity variation. The viscosity measurement was not attempted however, the slight variation in the trend corresponding to each of the experiment indicate the potential variation in the viscosity. The initial rapid movement of the flow front can be due to the resin flow in the linear direction, subsequent reduction in the velocity can be since the resin progression also occurred in the transverse direction through the fiber layers. The same was confirmed in the microscopic analysis (Fig. 4 b) where the RTM6 resin flow was observed through the reinforcement fiber layer and in the inter-tow regions of the fiber bundle.

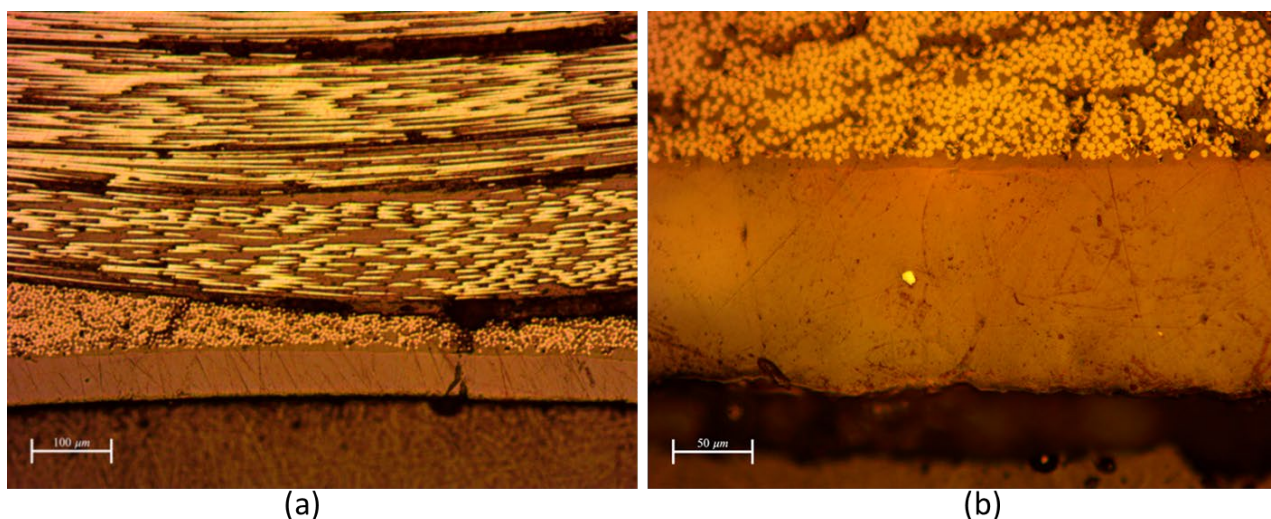


Fig. 4 The cross-sectional optical micrograph after the resin infusion depicting (a) the resin flow though the fiber plies, magnification 10x. (b) presence of hybrid interlayer, magnification 20x.

**Analysis of metallized hybrid composites.** Influence of the cold spraying process parameters gas temperature and the SoD was investigated at the constant chamber pressure of 5.5 bar. The substrate side which was exposed for the CS pass contained the PEI layer rendering it feasible to produce a AlSi10Mg coating after experiencing the polymer softening at T3 and T4 temperatures.



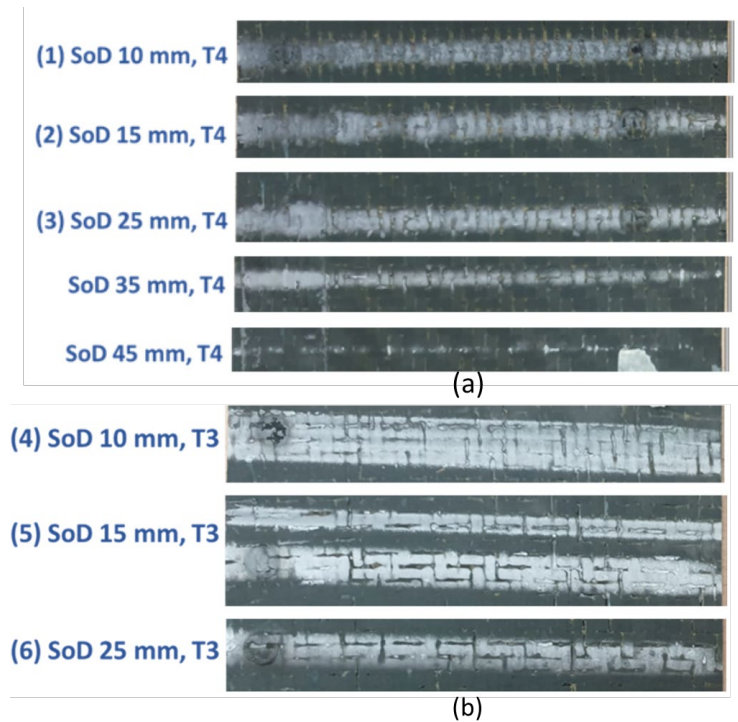


Fig. 5 (a) and (b) Cold sprayed panel with the enlsted process parameters.

Metallization attempt at the lowest temperature T2 with SoD variation did not result in significant coating (not included in the image). It can be attributed to the insufficient heat generation at lower gas temperature. Increasing the gas temperature (T3) it was possible to attain double passes as visible from the Fig. 5 (b) SoD 10 mm case. Opportune setting of the gas temperature and the SoD ensured the sufficient velocity of the impinging coating particles and the substrate heating to facilitate the entrapment sites. Increase in SoD to 15 and 25 mm led to higher polymer softening in the inter-tow regions and powder dispersion. Further increase in the gas temperature (T4) yielded a continuous coating formation except in the cases where the SoD was highest i.e., 35, 45 mm SoD. Non uniform width coating was formed over the substrate specifically evident for the SoD 45 mm and gas temperature T4 (Fig. 5 (a)). In such cases, it can be assumed that though the gas temperature was high enough to ensure the substrate heating, the increased SoD resulted in the heat losses as well as reduction in the coating powder velocity.

The resultant CS panels were subjected to the SEM microstructural analysis to assess the spraying features. As shown in Fig. 6 (a) the coating layer exhibited the inconsistent thickness and detachment from several sites. Primary reason behind such irregularities can be in relation to the extensive metallographic preparation. Metallic coating layer was removed in several places in preparation. To understand if the derived layer was indeed part of the cold spraying pass, EDAX analysis was followed by the SEM. Three different electron spectra (numbered 6,7, and 8 in Fig. 6) were obtained in the random positions over the coated layer.

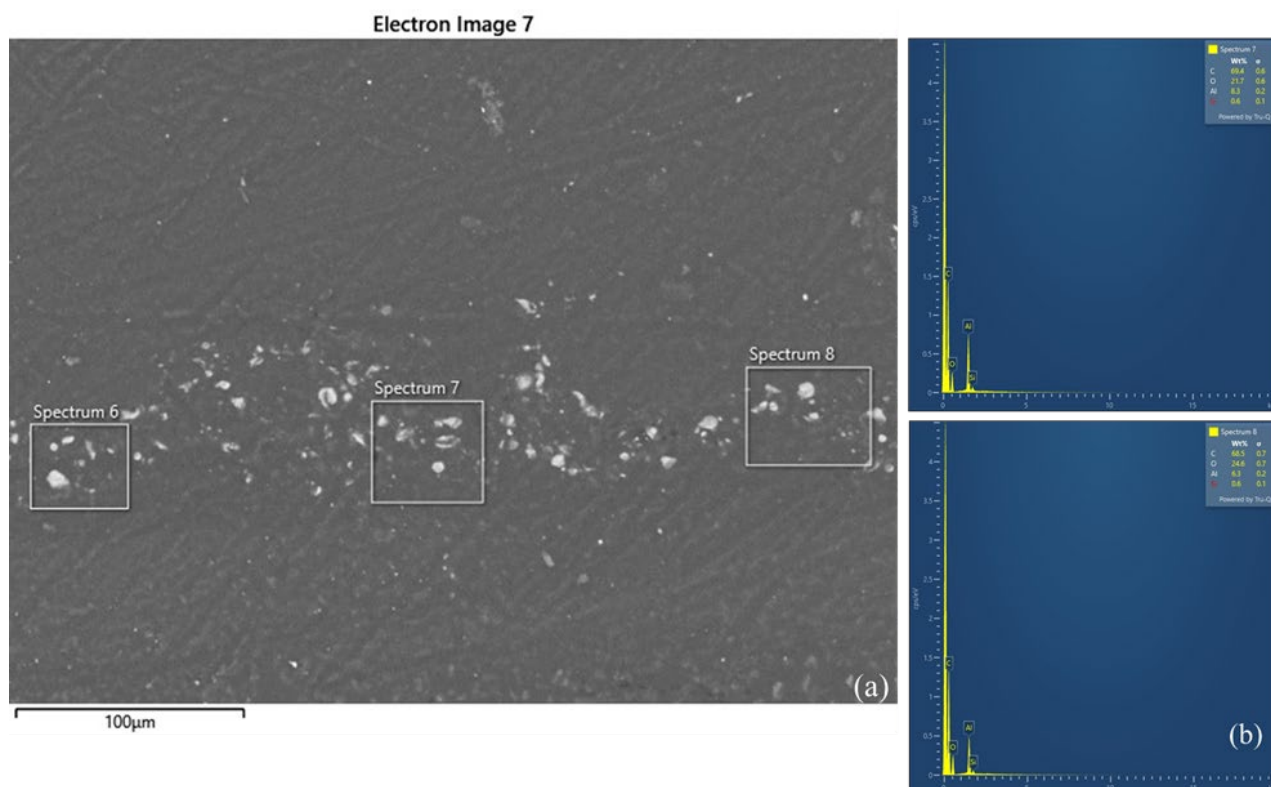


Fig. 6 (a) SEM micrograph acquired for the coating conditions of SoD 15 mm, T3 300°C temperature in the cross-sectional direction and highlighting the coating areas and (b) EDAX spectra for the elemental composition determination and correlating with the SEM micrographs.

The EDAX spectrums (numbered 7 and 8 in Fig. 6 (b, c)) exhibited the presence of the Al, and Si elements, originally the coating constituents. Higher amount of these elements indicates the presence of intact coating on certain areas of the specimen.

**Adhesion test.** The adhesion pull-off tests were conducted on the specimen coated under varying process parameters condition and the similar manufacturing condition. Referring to the circular impression formed over the coated adherend in the Fig. 7, adhesion strength values were derived upon the detachment of the stub positioned over the adherend covered with adhesive. The detachment upon failure left the visible circular impression on the substrate (Fig. 5) and stub surface in some cases displayed substrate residue (Fig. 8 b, c). The adhesion tests were not feasible in the insufficient coating layer thickness condition i.e., the SoD 35 and 45 mm with T4 gas temperature. The obtained adhesion strength for each spot differed according to the sprayed processing parameters as reported in the Fig. 7.

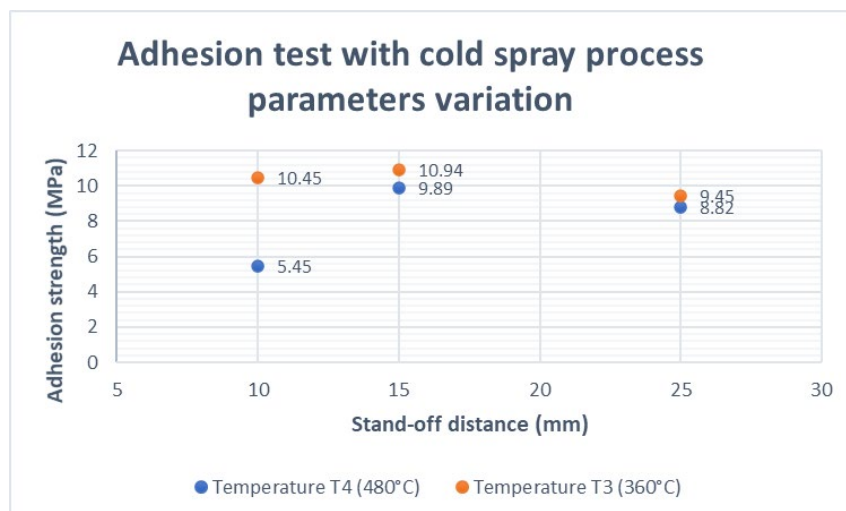


Fig. 7 Adhesion trend corresponding to the various cold spray conditions.

Inferior adhesion strength for all the T4 temperature cases can be ascribed to the higher PEI substrate layer softening and damage as well as influence of the SoD which led to the coating particles scattered over the surface without the stronger interlocking. As indicated in the Fig. 7, the adhesion strength improvement was noted in the case of the opportune set of cold spraying processing parameter condition, i.e., T3 temperature and the intermediate SoD. Higher SoD can reduce the particle velocity producing a loosely bound coating which yielded poor adhesion.

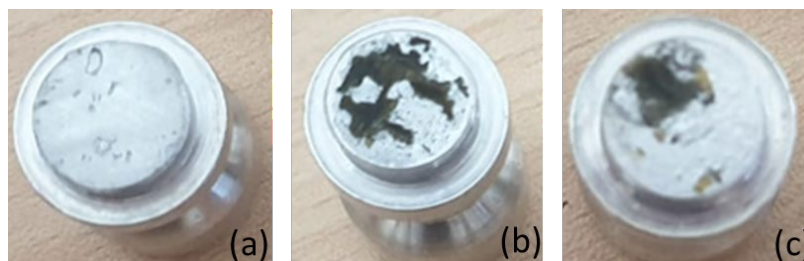


Fig. 8 The pull stub surface post the pull-off test on (a) uncoated specimen (b) cold spraying condition of T3, 10 mm SoD (c) cold spraying condition of T4, 10 mm SoD.

In the conditions involving the T3 and T4 temperatures, the failure after the pull off test was observed from the adherend side suggesting the cohesive mode of failure. Different amount of the fiber residue content from substrates (Fig. 8 b, c) remained on the dolly surface, which indicated the contact between the adhesive and the substrate on certain spots as opposed to the ideal condition of adhesive contact with solely coating. Hence, the representative adhesion strength values indicated in the Fig. 7 are not solely corresponding to the adhesion strength of the coating. It can be considered as the cumulative adhesion strength of the substrate as well as coating.

Moreover, manufacturing condition exhibits important role in the obtained adhesion between the hybrid composite adherend and the coating surface. The higher adhesion between the PEI layer and the remaining part of the substrate was evident from the detached stub as shown in the Fig. 8 (a). Adhesive mode of failure was observed in the case of the uncoated specimen. The dolly surface depicted no sign of PEI layer, fiber residue from the substrate or any adhesive attachment. This indicated presence of stronger adhesion between the PEI layer and the substrate. Comparative to the metallized substrates, adhesion strength of 3.5 MPa for the uncoated substrate was obtained (not mentioned in the graph).

## Summary

Following conclusions have been drawn from the investigation encompassing the hybrid interlayer method for the thermoset-thermoplastic composite formation and metallization;

- (1) Partially impregnated hybrid PEI and CF interlayer was formed by the hot-pressing action. Novel hybrid interlayer method was found suitable for manufacturing of hybrid composite panels in the VARI process route.
- (2) The AlSi10Mg powder coating by LPCS was found to be feasible on the hybrid thermoplastic thermoset fiber reinforced composites. Gas temperature as a process parameter was found to influence the coating formation since the intermediate temperature (T3) and SoD process parameter combination resulted in the improved coating formation and adhesion strength. In case of non-coated hybrid composite, adhesive mode of failure with no sign of PEI layer, fiber residue from the substrate indicated presence of stronger adhesion between the PEI layer and the substrate.

## Acknowledgement

This research has received funding from the Italian Project, PRIN2017: Cold Spray of Metal-to-Composite (COSMEC), ministerial code 2017N4422T\_001. The authors also acknowledge the industrial support from SOPHIA TECH industrial unit for facilitating the cold spraying experimentation.

---

## References

- [1] R.M.F. Paulo, F. Rubino, R.A.F. Valente, F. Teixeira-Dias, P. Carlone, Modelling of friction stir welding and its influence on the structural behaviour of aluminium stiffened panels, *Thin-Walled Struct.* 157 (2020) 107128. <https://doi.org/10.1016/j.tws.2020.107128>.
- [2] F. Rubino, H. Parmar, V. Esperto, P. Carlone, Ultrasonic welding of magnesium alloys: a review, *Mater. Manuf. Process.* 35 (2020) 1051–1068. <https://doi.org/10.1080/10426914.2020.1758330>.
- [3] F. Rubino, M. Pisaturo, A. Senatore, P. Carlone, T.S. Sudarshan, Tribological Characterization of SiC and B4C Manufactured by Plasma Pressure Compaction, *J. Mater. Eng. Perform.* 26 (2017) 5648–5659. <https://doi.org/10.1007/s11665-017-3016-9>.
- [4] F. Rubino, P. Poza, G. Pasquino, P. Carlone, Thermal spray processes in concentrating solar power technology, *Metals (Basel)*. 11 (2021) 1–30. <https://doi.org/10.3390/met11091377>.
- [5] H. Parmar, T. Khan, F. Tucci, R. Umer, P. Carlone, Advanced robotics and additive manufacturing of composites: towards a new era in Industry 4.0, *Mater. Manuf. Process.* (2021). <https://doi.org/10.1080/10426914.2020.1866195>.
- [6] A. Viscusi, Numerical investigations on the rebound phenomena and the bonding mechanisms in cold spray processes, *AIP Conf. Proc.* 1960 (2018). <https://doi.org/10.1063/1.5034957>.
- [7] A. Viscusi, A. Astarita, L. Carrino, G. D'Avino, C. de Nicola, P.L. Maffettone, G.P. Reina, S. Russo, A. Squillace, Experimental study and numerical investigation of the phenomena occurring during long duration cold spray deposition, *Int. Rev. Model. Simulations*. 11 (2018) 84–92. <https://doi.org/10.15866/iremos.v11i2.13619>.
- [8] A. Formisano, A. Barone, L. Carrino, D. De Fazio, A. Langella, A. Viscusi, M. Durante, Improvement of the mechanical properties of reinforced aluminum foam samples, *AIP Conf. Proc.* 1960 (2018). <https://doi.org/10.1063/1.5034947>.
- [9] A.T. Silvestri, I. Papa, F. Rubino, A. Squillace, On the critical technological issues of CFF: enhancing the bearing strength, *Mater. Manuf. Process.* 00 (2021) 1–13. <https://doi.org/10.1080/10426914.2021.1954195>.
- [10] A.T. Silvestri, A. Astarita, A. El Hassanin, A. Manzo, U. Iannuzzo, G. Iannuzzo, V. de Rosa, F. Acerra, A. Squillace, Assessment of the mechanical properties of AlSi10Mg parts produced through selective laser melting under different conditions, *Procedia Manuf.* 47 (2020) 1058–1064. <https://doi.org/10.1016/j.promfg.2020.04.115>.
- [11] A. El Hassanin, F. Scherillo, A.T. Silvestri, A. Caraviello, R. Sansone, A. Astarita, A. Squillace, Heat treatment of inconel selective laser melted parts: Microstructure evolution, *AIP Conf. Proc.* 2113 (2019). <https://doi.org/10.1063/1.5112599>.
- [12] I. Papa, A.T. Silvestri, M.R. Ricciardi, V. Lopresto, A. Squillace, Effect of fibre orientation on novel continuous 3d-printed fibre-reinforced composites, *Polymers (Basel)*. 13 (2021). <https://doi.org/10.3390/polym13152524>.
- [13] A. El Hassanin, M. Troiano, F. Scherillo, A.T. Silvestri, V. Contaldi, R. Solimene, F. Scala, A. Squillace, P. Salatino, Rotation-assisted abrasive fluidised bed machining of alsi10mg parts made through selective laser melting technology, *Procedia Manuf.* 47 (2020) 1043–1049. <https://doi.org/10.1016/j.promfg.2020.04.113>.
- [14] A. El Hassanin, M. Troiano, A.T. Silvestri, V. Contaldi, F. Scherillo, R. Solimene, F. Scala, A. Squillace, P. Salatino, Influence of abrasive materials in fluidised bed machining of AlSi10Mg parts made through selective laser melting technology, *Key Eng. Mater.* 813 KEM (2019) 129–134. <https://doi.org/10.4028/www.scientific.net/KEM.813.129>.



- 
- [15] A. El Hassanin, C. Velotti, F. Scherillo, A. Astarita, A. Squillace, L. Carrino, Study of the solid state joining of additive manufactured components, RTSI 2017 - IEEE 3rd Int. Forum Res. Technol. Soc. Ind. Conf. Proc. (2017). <https://doi.org/10.1109/RTSI.2017.8065967>.
- [16] F. Tucci, R. Bezerra, F. Rubino, P. Carlone, Multiphase flow simulation in injection pultrusion with variable properties, *Mater. Manuf. Process.* 35 (2020) 152–162. <https://doi.org/10.1080/10426914.2020.1711928>.
- [17] M.R. Rokni, P. Feng, C.A. Widener, S.R. Nutt, Depositing Al-Based Metallic Coatings onto Polymer Substrates by Cold Spray, *J. Therm. Spray Technol.* 28 (2019) 1699–1708. <https://doi.org/10.1007/s11666-019-00911-y>.
- [18] X.L. Zhou, A.F. Chen, J.C. Liu, X.K. Wu, J.S. Zhang, Preparation of metallic coatings on polymer matrix composites by cold spray, *Surf. Coatings Technol.* 206 (2011) 132–136. <https://doi.org/10.1016/j.surfcoat.2011.07.005>.
- [19] M. Grujicic, C.L. Zhao, W.S. DeRosset, D. Helfrich, Adiabatic shear instability based mechanism for particles/substrate bonding in the cold-gas dynamic-spray process, *Mater. Des.* 25 (2004) 681–688. <https://doi.org/10.1016/j.matdes.2004.03.008>.
- [20] H. Parmar, F. Tucci, P. Carlone, T.S. Sudarshan, Metallisation of polymers and polymer matrix composites by cold spray: state of the art and research perspectives, *Int. Mater. Rev.* (2021) 1–25. <https://doi.org/10.1080/09506608.2021.1954805>.
- [21] R. Della Gatta, A. Viscusi, A.S. Perna, A. Caraviello, A. Astarita, Cold spray process for the production of AlSi10Mg coatings on glass fibers reinforced polymers, *Mater. Manuf. Process.* 36 (2021) 106–121. <https://doi.org/10.1080/10426914.2020.1813895>.
- [22] A. Ganesan, M. Yamada, M. Fukumoto, Cold spray coating deposition mechanism on the thermoplastic and thermosetting polymer substrates, *J. Therm. Spray Technol.* 22 (2013) 1275–1282. <https://doi.org/10.1007/s11666-013-9984-x>.
- [23] A. Ganesan, J. Affi, M. Yamada, M. Fukumoto, Bonding behavior studies of cold sprayed copper coating on the PVC polymer substrate, *Surf. Coatings Technol.* 207 (2012) 262–269. <https://doi.org/10.1016/j.surfcoat.2012.06.086>.
- [24] A. Małachowska, M. Winnicki, M. Stachowicz, M. Korzeniowski, Metallisation of polycarbonates using a low pressure cold spray method, *Surf. Eng.* 34 (2018) 251–258. <https://doi.org/10.1080/02670844.2016.1277843>.
- [25] H. Che, X. Chu, P. Vo, S. Yue, Metallization of Various Polymers by Cold Spray, *J. Therm. Spray Technol.* 27 (2018) 169–178. <https://doi.org/10.1007/s11666-017-0663-1>.
- [26] M. Gardon, A. Latorre, M. Torrell, S. Dosta, J. Fernández, J.M. Guilemany, Cold gas spray titanium coatings onto a biocompatible polymer, *Mater. Lett.* 106 (2013) 97–99. <https://doi.org/10.1016/j.matlet.2013.04.115>.
- [27] V. Gillet, E. Aubignat, S. Costil, B. Courant, C. Langlade, P. Casari, W. Knapp, M.P. Planche, Development of low pressure cold sprayed copper coatings on carbon fiber reinforced polymer (CFRP), *Surf. Coatings Technol.* 364 (2019) 306–316. <https://doi.org/10.1016/j.surfcoat.2019.01.011>.
- [28] F. Rubino, F. Tucci, V. Esperto, A.S. Perna, A. Astarita, P. Carlone, A. Squillace, Metallization of Fiber Reinforced Composite by Surface Functionalization and Cold Spray Deposition, *Procedia Manuf.* 47 (2020) 1084–1088. <https://doi.org/10.1016/j.promfg.2020.04.353>.
- [29] A.S. Perna, A. Astarita, P. Carlone, X. Guthmann, A. Viscusi, Characterization of Cold-Spray Coatings on Fiber-Reinforced Polymers through Nanoindentation Tests, *Metals (Basel)*. 11 (2021) 331. <https://doi.org/10.3390/met11020331>.

- 
- [30] J. Affi, H. Okazaki, M. Yamada, M. Fukumoto, Fabrication of aluminum coating onto CFRP substrate by cold spray, *Mater. Trans.* 52 (2011) 1759–1763. <https://doi.org/10.2320/matertrans.T-M2011807>.
- [31] F. Rubino, F. Tucci, V. Esperto, A.S. Perna, A. Astarita, P. Carlone, A. Squillace, Metallization of Fiber Reinforced Composite by Surface Functionalization and Cold Spray Deposition, in: 23rd Int. Conf. Mater. Form. (ESAFORM 2020), 2019.
- [32] E. Tsiangou, S. Teixeira de Freitas, I. Fernandez Villegas, R. Benedictus, Investigation on energy director-less ultrasonic welding of polyetherimide (PEI)- to epoxy-based composites, *Compos. Part B Eng.* 173 (2019) 107014. <https://doi.org/10.1016/j.compositesb.2019.107014>.
- [33] I.F. Villegas, R. van Moorlehem, Ultrasonic welding of carbon/epoxy and carbon/PEEK composites through a PEI thermoplastic coupling layer, *Compos. Part A Appl. Sci. Manuf.* 109 (2018) 75–83. <https://doi.org/10.1016/j.compositesa.2018.02.022>.
- [34] H. Parmar, A. Gambardella, A.S. Perna, A. Viscusi, R. Della Gatta, F. Tucci, A. Astarita, P. Carlone, Manufacturing and metallization of hybrid thermoplastic-thermoset matrix composites, *ESAFORM 2021*. (2021). <https://doi.org/10.25518/esaform21.2727>.